ChemComm

Accepted Manuscript

This article can be cited before page numbers have been issued, to do this please use: H. Yang, Q. Lin, H. Zhang, G. Li, L. Fan, X. Chai, Q. Zhang, J. Liu and C. He, *Chem. Commun.*, 2018, DOI: 10.1039/C8CC00969D.

ROYAL SOCIETY OF CHEMISTRY

rsc.li/chemcomm

View Article Online
DOI: 10.1039/C8CC00969D

Chemical Communications

COMMUNICATION

Platinum/nitrogen-doped carbon/carbon cloth: a bifunctional catalyst for electrochemical reduction and carboxylation of CO_2 with excellent efficiency

Received 00th January 20xx,
Accepted 00th January 20xx

DOI: 10.1039/x0xx00000x

www.rsc.org/

Heng-Pan Yang, Qing Lin, Han-Wen Zhang, Guo-Dong Li, Liang-Dong Fan, Xiao-Yan Chai, Qian-Ling Zhang, Jian-Hong Liu and Chuan-Xin He*

A novel Pt-NPs@NCNFs@CC composite was prepared by electrospinning technique. It was a highly efficient and binder-free catalyst for CO_2 direct reduction and carboxylation with halides. Formate with 91% Faradaic efficiency and 2-phenylpropionic acid with 99% yield could be obtained, respectively. Moreover, this catalyst has excellent stability and reusability.

Concerned about CO_2-triggered climate issues, scientists have made great efforts working on CO_2 capture, storage and utilization.[1, 2] Since CO_2 is also a nontoxic, ubiquitous and sustainable C1 resource, it is very attractive to convert CO_2 into useful compounds by chemical fixation.[3-7] The carboxylation of CO_2 with organic compounds,[8-10] like aryl halides, olefins and alcohols, is an alternative choice for chemical fixation of CO_2, which always involves transition-metal complex as catalysts. The as-synthesized carboxylic acids is highly valuable, since they are common structural motifs in bioactive molecules.[11, 12]

Besides carboxylation, electrochemical reduction of CO_2 to small molecule compounds also attracts wide attention. The main hurdle for this technology is the availability of efficient and robust catalysts, since CO_2 itself is very stable and relatively inert. For the last three decades, a range of catalysts including metals and their oxides,[6, 7] small molecules (especially nitrogen heterocyclic molecules),[13, 14] covalent organic frameworks (COF),[15] metal-organic frameworks (MOFs),[16] and nitrogen-doped carbons[17] have been explored for electrochemical reduction of CO_2, conquering the challenges in poor efficiency and selectivity, lack of stability, recycling ability and low productivity. In an effort to solve the above issues, we formerly prepared a series of organically doped metal composites by the entrapment of homogeneous pyridine derivative (PYD) within metal or alloy nanoparticles, which could selectively reduce CO_2 to specific products with excellent stability and reusability. What's more, we demonstrated that pyridine nitrogen with the assistance of metallic platinum was efficient for electrochemical reduction of CO_2.[18-20]

In this work, we prepared a novel composite material (Pt-NPs@NCNFs@CC) by electrospinning of nitrogen-doped carbon nanofibers (NCNFs), embedding with platinum nanoparticles (Pt NPs), onto flexible carbon cloth (CC). N-doped carbon materials have been widely applied in electro-catalysis, the production of which always involves the utilization of polymer binders to make them useful as practical electrodes, but they are almost entirely powder-based and suffer from low productivity.[21] It's notable that carbon cloth was used as the conductive collecting substrate in the electrospinning process and carrier for fragile Pt-NPs@NCNFs, hence our Pt-NPs@NCNFs@CC catalyst didn't need powdering or binding to specific supports. What's more, Pt-NPs@NCNFs@CC contains pyridine nitrogen and metallic platinum, which might be potential active sites for electrochemical reduction of CO_2.

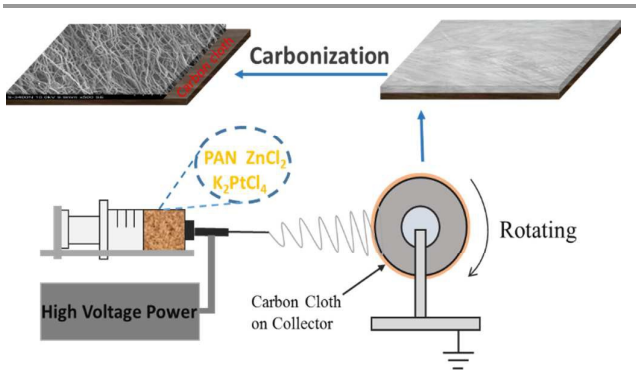

Fig. 1 Schematic illustration of the synthesis of Pt-NPs@NCNFs@CC.

Fig. 1 illustrate the fabrication procedure of Pt-NPs@NCNFs@CC. Briefly, a precursor solution with specific

Department of Chemistry, College of Chemistry and Environmental Engineering, Shenzhen University, Shenzhen, Guangdong, 518060, China
**Corresponding Author: Prof. Chuan-Xin He (Tel: +86 0755-26536141, E-mail: hecx@szu.edu.cn).*
Electronic Supplementary Information (ESI) available: materials, instruments, general methods, characterization of electrolysis products, stability test of Pt-NPs@NCNFs@CC, synthesis and characterization of different cathodes. See DOI: 10.1039/x0xx00000x

View Article Online
DOI: 10.1039/C8CC00969D

weight ratio of polyacrylonitrile (PAN), K_2PtCl_4 and $ZnCl_2$ in N, N-dimethylformamide (DMF) was prepared and sucked into a syringe. Electrospinning of the as-prepared solution was performed under 21 kV with a vertically positioned carbon cloth as collector. After carbonization at 800 °C in argon atmosphere, the PAN molecules were decomposed and converted into N-doped carbon materials. Meanwhile, the Pt^{2+} species were reduced to metallic Pt-NPs. The Zn^{2+} species were reduced to metallic Zn, which would further vaporize at high temperatures, resulting in the generation of the porous structure in NCNFs. Details about the preparation of Pt-NPs@NCNFs@CC and other catalysts as contrast were provided in the support information. This porous structure was investigated through N_2 adsorption-desorption measurements (Fig. S1). It can be found that the specific surface area of Pt-NPs@NCNFs@CC was 233.5 $m^2\ g^{-1}$, significant larger than that without any $ZnCl_2$ in precursor solution (9.6 $m^2\ g^{-1}$). The corresponding pore-size-distribution curve shows that the size of the majority of the pores falls in the range of 4 nm to 5 nm (Fig. S1). The above results demonstrated the importance of the introduction of $ZnCl_2$ to create a porous structure.

X-Ray Diffraction (XRD) patterns confirmed the structure and composition of Pt-NPs@NCNFs@CC. As shown in Fig. 2A, diffraction peaks centered at 24.1° and 44.1° could be indexed to (002) and (100) planes of carbon cloth, respectively; no extra diffraction peaks were observed in this XRD pattern (Fig. 2A, a). As for Pt-NPs@NCNFs@CC (Fig. 2A, b), besides the diffraction peaks locating at 24.1° and 44.1°, three new strong peaks emerged at 39.8°, 46.3° and 67.6°, which could be ascribed to the facets (111), (200) and (220) of the face-centered-cubic (fcc) crystalline Pt, respectively. Much weaker diffraction peaks at 24.1° and 44.1° were observed in pure NCNFs (Fig. 2A, c), which might explain the absence of NCNFs diffraction peaks in Fig. 2A, b. From the above results, it can be verified that the as-spun fibers were indeed carbonized and Pt species were successfully reduced to the metallic state. The surface morphology and the interior structure of Pt-NPs@NCNFs@CC were characterized by multiple methods. According to the field-emission scanning electron microscopy (FE-SEM) images, the surface of the pristine carbon cloth was coated with a layer of three-dimensional nanofiber web after electrospinning (Fig. 2B) compared with pure carbon cloth, leading to an obvious color change of the fabric from grey to dark balck (Fig. S2). Importantly, we found that these nanofibers were partially inserted in the carbon cloth after scraping away the nanofiber layer (Fig. S2), which revealed the stable immobilization of Pt-NPs@NCNFs onto the carbon cloth surface. The diameters of the nanofibers were in the range of 400 nm to 600 nm (Fig. 2C, D). Notably, almost no trace of Pt-NPs was observed on the nanofiber surface. As for high-resolution transmission electron microscope (HR-TEM) analysis, it can be observed that the vast majority of nanoparticles are embedded within the nanofibers. The observed Pt-NPs had an average diameter of 5 nm, showing no trend to aggregate (Fig. 2D, E). The lattice distance as marked with the red arrows was measured as 2.3 Å, corresponding to the (111) plane of Pt fcc crystal (Fig. 2E). The selected area electron diffraction (SAED, inset of Fig. 2E) image of Pt-NPs@NCNFs@CC demonstrated the ring patterns assigned to (111), (200) and (220) plane of Pt fcc crystal, showing the polycrystalline nature of Pt, which was in agreement with the XRD pattern. Moreover, Fig. S3 and Fig. 2F showed the energy dispersive X-Ray spectroscopy (EDX) mapping images of Pt-NPs@NCNFs. The good match between C, N and Pt elements confirmed the homogeneous distribution of doped nitrogen and Pt-NPs within the nanofibers. X-ray photoelectron spectroscopy (XPS) was illustrated in Fig. S3. Three peaks of C 1s located at 284.7 eV, 285.2 eV and 286.2 eV were corresponded to C-C, C=N and C-N bonds, respectively. Furthermore, N 1s spectra was fitted into two peaks at 398.8 eV and 401.2 eV, assignable to pyridinic N atoms (61.5 at%) and graphitic N atoms (38.5 at%), respectively. The Pt 4f XPS spectrum contained two sharp peaks at around 71.5 eV (Pt $4f_{7/2}$) and 74.4 eV (Pt $4f_{5/2}$), which was corresponded with Pt^0.

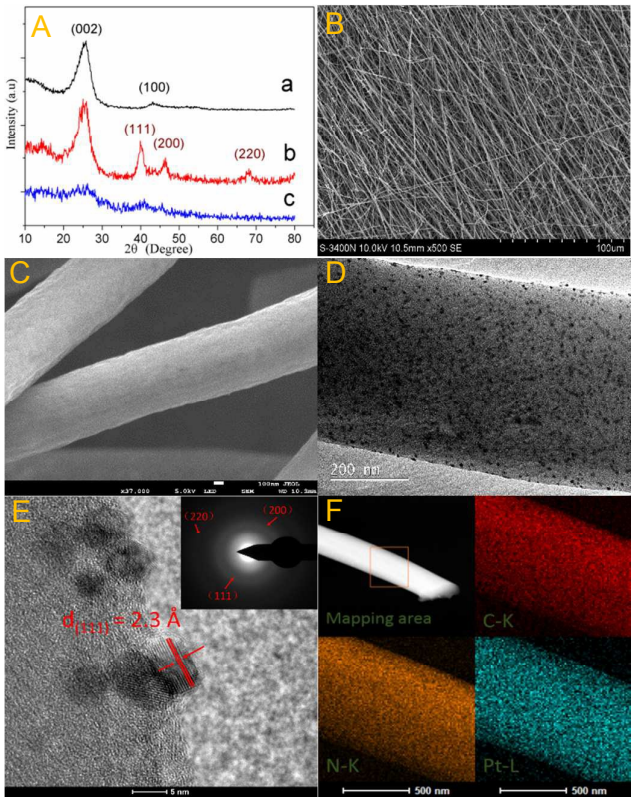

Fig. 2: Characterization of Pt-NPs@NCNFs@CC. A: XRD patterns of CC (a), Pt-NPs@NCNFs@CC (b) and NCNFs (c); FE-SEM patterns (B, C) and HR-TEM images (D, E) of Pt-NPs@NCNFs@CC, the inset shows the SAED images; EDX mapping (F) of Pt-NPs@NCNFs@CC.

According to the analysis above, the Pt-NPs@NCNFs@CC we prepared contains abundant, even-distributed pyridinic nitrogen and Pt-NPs. According to former reports, pyridinic nitrogen with the assistance of Pt is efficient catalysts for electrocatalytic CO_2 reduction. To evaluate the electrochemical ability of Pt-NPs@NCNFs@CC for CO_2 reduction, linear sweep voltammetry test was first performed in CO_2 or N_2 saturated 0.1 M $KHCO_3$ solution. As shown in Fig. 3A, obviously higher reductive current was observed at the Pt-NPs@NCNFs@CC

View Article Online
DOI: 10.1039/C8CC00969D

electrode under CO_2 atmosphere than under N_2 atmosphere, demonstrating that CO_2 can be electrochemically reduced by Pt-NPs@NCNFs@CC. The onset potential for CO_2 reduction is -0.4 V_{RHE} at the Pt-NPs@NCNFs@CC electrode while lower than -0.7 V_{RHE} at the pure CC cathode by comparison (Fig. 3B). And the reductive current (around -0.4 V_{RHE}) achieved at the CC cathode was negligible compared to that at the Pt-NPs@NCNFs@CC electrode. Thus, the presence of Pt-NPs@NCNFs favours the electroreduction of CO_2.

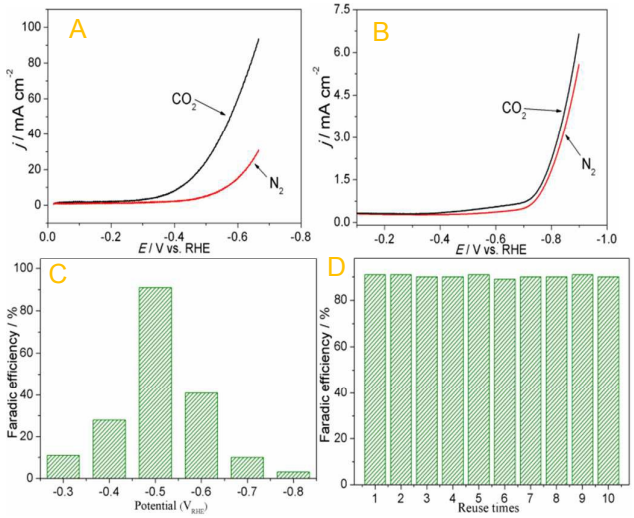

Fig. 3 LSV recorded at a sweep rate of 0.1 V s^{-1} in 0.1 M $KHCO_3$ solution at the Pt-NPs@NCNFs@CC (A) and CC (B) electrode; C: Faradaic efficiency for products using Pt-NPs@NCNFs@CC electrode at potentials from -0.3 to -0.8 V_{RHE}, charge: 100 C, anode: Pt foil, 20 mL CO_2-saturated 0.1 M $KHCO_3$ solution, temperature: 25 °C; D: reuse test of Pt-NPs@NCNFs@CC at -0.5 V_{RHE}.

The performance of the Pt-NPs@NCNFs@CC catalyst during CO_2 electroreduction was further examined by conducting constant-potential electrolysis in CO_2 saturated 0.1 M $KHCO_3$ solution. The applied potential for electrolysis was selected in the range of -0.3 to -0.8 V_{RHE} based on the onset potential at Pt-NPs@NCNFs@CC. The Pt-NPs@NCNFs@CC was cut into specific shapes and directly utilized as working electrode without the need of any binder. The liquid products were firstly detected qualitatively by ^{1}H NMR spectroscopy, which revealed that formate was obtained (Fig. S6, left). Gas chromatography (GC) showed that formate was the dominating product, reaching a maximum Faradaic efficiency of 91% at -0.5 V_{RHE} (Fig. 3C). What' more, after previous electrolysis, the Pt-NPs@NCNFs@CC cathode could be easily washed with water and then reused for a next reaction. The Faradaic efficiency of formate could maintain around 90% for at least 10 times (Fig. 3D). We also tested the long-term performance of Pt-NPs@NCNFs@CC at a constant cathode potential of -0.5 V_{RHE} for 30 h. The current density was kept around 40 mA cm^{-2} throughout the test (Fig. S6). The Pt-NPs@NCNFs@CC catalyst showed remarkable stability as well as reusability during the test.

To further understand the active sites of Pt-NPs@NCNFs@CC, a series of contrast experiments were also performed. Under the same conditions as that of Pt-NPs@NCNFs@CC, carbon cloth could not produce formate (Table S1, entry 7), hence the generation of formate was attributed to Pt-NPs@NCNFs. As mentioned before, metallic Pt with the assistance of pyridinic nitrogen might catalyze the electroreduction of CO_2. In our contrast experiments, pure Pt NPs could not produce formate (Table S1, entry 8), and NCNFs@CC produced formate with a Faradaic efficiency of only 8%, much lower than that of Pt-NPs@NCNFs@CC. Several catalysts with different amount of Pt NPs (Fig. S4, NCNFs@CC< Pt-NPs@NCNFs@CC-10< Pt-NPs@NCNFs@CC< Pt-NPs@NCNFs@CC-40) and pyridinic nitrogen (Fig. S5, Pt-NPs@NCNFs@CC-900< Pt-NPs@NCNFs@CC-700< Pt-NPs@NCNFs@CC) were also synthesized as contrast. Under the same conditions, formate with 8%, 73%, 91% and 91% Faradaic efficiency could be achieved at the NCNFs@CC, Pt-NPs@NCNFs@CC-10, Pt-NPs@NCNFs@CC and Pt-NPs@NCNFs@CC-40 cathode (Table S1, entry 2, 3, 1 and 4), respectively, revealing that the increase of Pt-NPs amount was in favour of the formation of formate. As for pyridinic nitrogen, formate with 76%, 80% and 91% Faradaic efficiency could be obtained at the Pt-NPs@NCNFs@CC-900, Pt-NPs@NCNFs@CC-700 and Pt-NPs@NCNFs@CC cathode (Table S1, entry 6, 5 and 1), respectively, which demonstrated the importance of pyridinic nitrogen in this procedure. We could conclude that the formation of formate with an excellent Faradaic efficiency was attributed to Pt NPs as well as pyridinic nitrogen.

Mechinasms about the N-doped carbons catalyzed CO_2 reduction have been reported in a few papers. Some researchers pointed out that CO_2 molecule was first adsorbed to the basic carbon atom adjacent to the pyridinic N, forming $*CO_2$ molecule and subsequently, the adsorbed $*CO_2$ was reduced and protonated to give *COOH (Scheme S1, step 1 and 2). In our experiment, the NCNFs@CC only produced formate with an 8% Faradaic efficiency, far less than that of Pt-NPs@NCNFs@CC under the same conditions, which revealed that Pt-NPs also participated in this procedure. Pt has a significantly lower hydrogen overpotential than the other cathodes did, leaving ample hydrogen atoms adsorbed on the electrode surface that can react with other species.[22] Based on the experimental results and previous reports, [21, 23] we proposed that CO_2 molecule was adsorbed to the carbon atom adjacent to the pyridinic N, combined with the Pt-H generated from the Pt suface to give *COOH (Scheme S1, step 1, 3 and 4), which was futher reducd to formate as the product.

As we introduced in the beginning, carboxylation with organic compounds is also an important method for CO_2 fixation as well as direct reduction, which could generate highly valuable products. The electrocatalytic carboxylation of CO_2 was carried out in 0.1 mol L^{-1} 1-phenylethyl bromide (**1a,** as model substrate) in 20 mL of acetonitrile (MeCN), with Pt-NPs@NCNFs@CC as the cathode and sacrificial magnesium (Mg) as the anode (Scheme 1). After electrolysis, the products were detected by ^{1}H NMR spectroscopy (Fig. S7) and high performance liquid chromatography (HPLC). The main product was detected as 2-phenylpropionic acid (**2a**), which was a crucial intermediate for the synthesis of nonsteroidal antiinflammatory drugs (NSAIDs). The influences of electric

View Article Online
DOI: 10.1039/C8CC00969D

charge (Q), current density and the solvent were investigated to optimize the yield of **2a**. The results were summarized in Table S2. Under optimized reaction conditions, **2a** with 99% yield and more than 99% selectivity was obtained (Table 1, entry 1) at the Pt-NPs@NCNFs@CC cathode. Pt-NPs@NCNFs@CC could be easily-recovered and all the reactions were conducted under room temperature and pressure. The yield and selectivity obtained at Pt-NPs@NCNFs@CC are even comparable to those achieved using homogeneous metal complex catalysts.[8, 9]

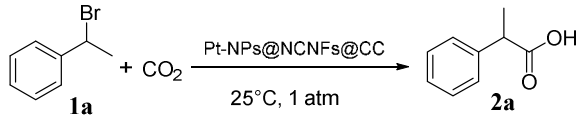

Scheme 1 Electro-carboxylation of CO_2 with **1a**.

Table 1 Electrochemical carboxylation of **1a** with CO_2 at different cathodes[a].

Entry	Cathode	Yield[b] (%)	Selectivity[b] (%)
1	Pt-NPs@NCNFs@CC	99	>99
2	NCNFs@CC	<1	-
3	CC	<1	-
4	Pt-NPs@NCNFs	97	>99
5	Pt-NPs/CC	32	84

[a] Anode: Mg, 20 mL CO_2-saturated MeCN, 0.1 M **1a**, supporting electrolyte: 0.1 M TEAI, current density: 3 mA cm^{-2}, charge: 2.5 F mol^{-1}, CO_2 pressure: 1 atm, 25 °C. [b] Determined by HPLC.

Similar results could also be achieved using Pt-NPs@NCNFs. In contrast, **2a** with less than 1% yield was detected under the same conditions using NCNFs@CC or CC as cathode, and **2a** with 32% yield and 84% selectivity was obtained at Pt-NPs/CC (Fig. S8). These phenomena indicated that Pt NPs are indispensable for the formation of **2a**. NCNFs alone could not produce **2a**, but they could adsorb CO_2 molecule and increase the CO_2 concentration around Pt NPs, which might account for the much higher yield obtained at Pt-NPs@NCNFs@CC than that of pure Pt NPs. Using reaction conditions of Table 1, entry 1, other benzyl halides were also tested for electro-carboxylation with CO_2. According to Fig. S7 and Table S3, Pt-NPs@NCNFs@CC could be applicable to the carboxylation of CO_2 with wide range of substrates. In addition, we also test the reusability of Pt-NPs@NCNFs@CC in CO_2 carboxylation under the same conditions as Table 1 entry 1, the yield of 2-phenylpropionic acid could maintain around 98% (Fig. S9).

After CO_2 reduction and carboxylation reactions, the Pt-NPs@NCNFs@CC cathode was characterized by multiple methods. N_2 adsorption-desorption measurement showed that Pt-NPs@NCNFs@CC still had a specific surface area of around 230 m^2 g^{-1}. According to the XRD, XPS and TEM patterns, the chemical composition of Pt-NPs@NCNFs@CC also didn't change (Fig. S10). In a word, our Pt-NPs@NCNFs@CC composite own remarkable stability and reusability, which are significant for practical applications.

In conclusion, Pt-NPs@NCNFs@CC, a highly efficient and binder-free catalyst was preparaed by electrospinning with the size of 25×28 cm at one time. Pt-NPs@NCNFs@CC could be directly used as cathode for electrochemical reduction as well as carboxylation of CO_2, for which formate with 91% Faradaic efficiency and 2-phenylpropionic acid with 99% yield could be obtained, respectively. Pt-NPs@NCNFs@CC also has remarkable stability and reusability, which might have practical applications in the future.

Notes and references

The financial support of the National Natural Science Foundation (NNSF) of China (21574084 and 21571131), the Natural Science Foundation of Guangdong Province (2015A030313554 and 2017A040405066), and Shenzhen Government's Plan of Science and Technology (JCYJ20160308104704791) are gratefully acknowledged.

1 J. Albo, M. Alvarez-Guerra, P. Castañoa, A. Irabienb, *Green Chem.,* 2015, **17**, 2304–2324.
2 J. Kim, T. A. Johnson, J. E. Miller, E. B. Stechel, C. T. Maravelias, *Energy Environ. Sci.,* 2014, **5**, 8417–8429.
3 L. Zhang, Z. Hou, *Chem. Sci.,* 2013, **4**, 3395–3403.
4 Y. Tsuji, T. Fujihara, *Chem. Commun.,* 2012, **48**, 9956–9964.
5 C. Costentin, M. Robert, J. M. Saveant, *Chem. Soc. Rev.,* 2013, **42**, 2423–2436.
6 K. P. Kuhl, E. R. Cave, D. N. Abram, T. F. Jaramillo, *Energy Environ. Sci.,* 2012, **5**, 7050–7059.
7 K. J. P. Schouten, Y. Kwon, C. J. M. van der Ham, Z. Qin, M. T. M. Koper, *Chem. Sci.,* 2011, **2**, 1902–1909.
8 T. Leon, A. Correa, R. Martin, *J. Am. Chem. Soc.,* 2013, **135**, 1221–1224
9 M. Börjesson, T. Moragas, D. Gallego, R. Martin, *ACS Catal.,* 2016, **6**, 6739–6749.
10 H. P. Yang, Y. N. Yue, Q. L. Sun, Q. Feng, H. Wang, J. X. Lu, *Chem. Commun.,* 2015, **51**, 12216–12219.
11 L. J. Goossen, N. Rodríguez, K. Gooßen, *Angew. Chem., Int. Ed.,* 2008, **47**, 3100–3120.
12 H. Maag, Prodrugs of Carboxylic Acids; Springer: New York, 2007.
13 G. Seshadri, C. Lin, A. B. Bocarsly, *J. Electroanal. Chem.,* 1994, **372**, 145–150.
14 E. B. Cole, P. S. Lakkaraju, D. M. Rampulla, A. J. Morris, E. Abelev, A. B. Bocarsly, *J. Am. Chem. Soc.,* 2010, **132**, 11539–11551.
15 S. Lin, C. S. Diercks, Y. B. Zhang, N. Kornienko, E. M. Nichols, Y. Zhao, A. R. Paris, D. Kim, P. Yang, O. M. Yaghi, C. J. Chang, *Science,* 2015, **349**, 1208–1213.
16 I. Hod, M. D. Sampson, P. Deria, C. P. Kubiak, O. K. Farha, J. T. Hupp, *ACS Catal.,* 2015, **5**, 6302–6309.
17 Y. Liu, S. Chen, X. Quan, H. Yu, *J. Am. Chem. Soc.,* 2015, **137**, 11631–11636.
18 H. P. Yang, S. Qin, H. Wang, J. X. Lu, *Green Chem.,* 2015, **17**, 5144–5148.
19 H. P. Yang, Y. N. Yue, S. Qin, H. Wang, J. X. Lu, *Green Chem.,* 2016, **18**, 3216–3220.
20 H. P. Yang, S. Qin, Y. N. Yue, L. Liu, H. Wang, J. X. Lu, *Catal. Sci. Technol.,* 2016, **6**, 6490–6494.
21 H. Wang, J. Jia, P. Song, Q. Wang, D. Li, S. Min, C. Qian, L. Wang, Y. F. Li, C. Ma, T. Wu, J. Yuan, M. Antonietti, G. A. Ozin, *Angew. Chem. Int. Ed.,* 2017, **56**, 7847–7852.
22 D. Xiang, D. Magana, R. B. Dyer, *J. Am. Chem. Soc.,* 2014, **136**, 14007–14010.
23 D. Guo, R. Shibuya, C. Akiba, S. Saji, T. Kondo, J. Nakamura, *Science,* 2016, **351**, 361–365.